

Upward Planar Drawings with Three and More Slopes

Jonathan Klawitter  and Johannes Zink 

Universität Würzburg, Würzburg, Germany

Abstract. We study upward planar straight-line drawings that use only a constant number of slopes. In particular, we are interested in whether a given directed graph with maximum in- and outdegree at most k admits such a drawing with k slopes. We show that this is in general NP-hard to decide for outerplanar graphs ($k = 3$) and planar graphs ($k \geq 3$). On the positive side, for cactus graphs deciding and constructing a drawing can be done in polynomial time. Furthermore, we can determine the minimum number of slopes required for a given tree in linear time and compute the corresponding drawing efficiently.

Keywords: upward planar · slope number · NP-hardness

1 Introduction

One of the main goals in graph drawing is to generate clear drawings. For visualizations of directed graphs (or digraphs for short) that model hierarchical relations, this could mean that we explicitly represent edge directions by letting each edge point upward. We may also require a planar drawing and, if possible, we would thus get an upward planar drawing. For schematic drawings, we try to keep the visual complexity low, for example by using only few different geometric primitives [28] – in our case few slopes for edges. If we allow two different slopes we get orthogonal drawings [14], with three or four slopes we get hexalinear and octilinear drawings [36], respectively. Here, we combine these requirements and study upward planar straight-line drawings that use only few slopes.

Upward planarity. An *upward planar drawing* of a digraph G is a planar drawing of G where every edge is drawn as a monotonic upward curve. We call G *upward planar* if it admits an upward planar drawing and *upward plane* if it is equipped with an upward planar embedding. Note that an upward planar embedding, given by the edge order around each vertex, is necessarily *bimodal*, that is, each cyclic sequence can be split into two contiguous subsequences of incoming edges and outgoing edges [14]. Di Battista and Tamassia [15] have shown that if a digraph is upward planar, then it also admits an upward planar straight-line drawing.

While upward planarity testing is an NP-complete problem for general digraphs [23], there exist several FPT algorithms [9, 19, 25] and polynomial-time algorithms for special classes, e.g., for single source digraphs [6], outerplanar digraphs [38], series-parallel digraphs [19], and triconnected digraphs [5]. If the embedding is given, upward planarity can be tested in polynomial time [5].

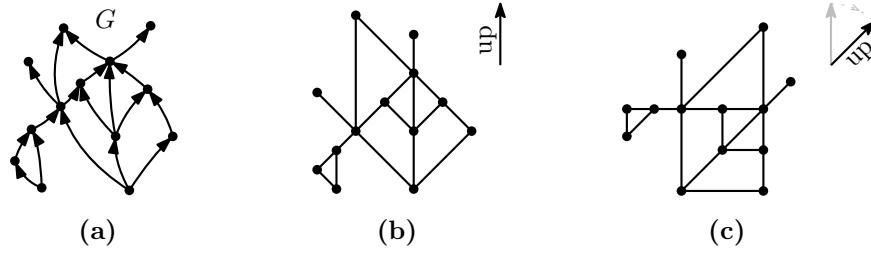


Fig. 1: (a) A digraph G with (b) upward planar 3-slope drawing; (c) drawing rotated by 45° . For readability, edge directions are now given implicitly.

k-slope drawings. A *k-slope drawing* of a (not necessarily directed) graph G is a straight-line drawing of G where every edge is drawn with one of at most k different slopes; see Fig. 1a–b. The *slope number* of G is the smallest k such that G admits a k -slope drawing. If only (upward) planar drawings are allowed, the number is called the (*upward*) *planar slope number* of G . The general and planar slope number have been studied extensively in the past for a variety of classes [8, 16, 17, 20, 21, 26, 27, 30, 32–34, 37, 41]. Recently, also the interest in upward planar drawings on few slopes has grown. For example, allowing one bend per edge, Bekos et al. [3] studied so-called bitonic *st*-graphs and complementarily Di Giacomo et al. [18] considered series-parallel digraphs. Brückner et al. [8] studied level-planar drawings with a fixed slope set. Older works include results by Czyzowicz et al. [12, 13] on lattices and several results for trees [1, 2, 7, 10].

In a companion paper to this one, Klawitter and Mchedlidze [29] show that it can be decided in linear time whether a given upward plane digraph admits an upward planar 2-slope drawing. For the variable embedding scenario and two slopes, they give a linear-time algorithm for single-source digraphs, a quartic-time algorithm for series-parallel digraphs, and an FPT algorithm for general digraphs.

Here, we study the problem of whether a digraph admits an upward planar k -slope drawing for any k – with a special focus on the next natural case $k = 3$. Clearly, we can presume that G has maximum in- and outdegree at most k . Note that a 2-slope drawing can be sheared in the direction of one slope without affecting the length of edges drawn with the other slope. The fact that this does not hold for three or more slopes introduces interesting new geometric aspects.

For the choice of k specific slopes, we propose three settings. In the *general* setting, any set of k distinct slopes can be chosen. In the *uniform (angles)* setting, we use slopes with angles in $\{i \cdot \pi/k \mid i \in \{0, \dots, k-1\}\}$ clockwise (cw) from the x-axis. In the *regular grid* setting, we define a set of slopes as follows. Let c be the middle grid point of a $W \times W$ square grid, where $W = 2\lceil \log_2 k \rceil - 1$. Pick any k distinct slopes that you get from connecting c to any of the other grid points. We remark that these slopes are contained in (an extended version of) the W -th Farey sequence¹. Uniform angles naturally lead to more balanced drawings

¹ The W -th Farey sequence is the sequence of all completely reduced fractions where the nominator and denominator is at most W in order of increasing size.

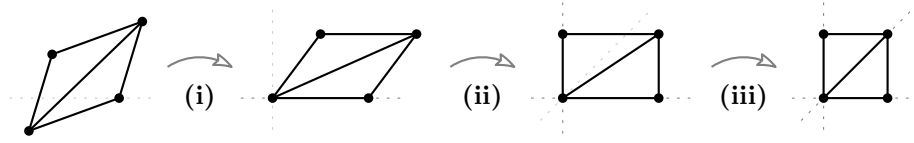


Fig. 2: Given a drawing using any set of three slopes, we can (i) rotate, (ii) shear, and (iii) scale it to only use the slope set $\{\uparrow, \nearrow, \rightarrow\}$.

with more rotational symmetry, which we find more visually appealing. The downside of this setting is that we cannot always use grid points of the regular 2D grid. E.g., for $k = 6$, the third slope is $\tan(\frac{2}{6}\pi) = \sqrt{3}$, which is an irrational number. Therefore, we assume henceforth for uniform angles a computation and representation model that can handle implicit coordinates or alternatively real numbers. On the other hand in the regular grid setting, we get unbalanced edge angles and irrational edge lengths. Since all of these settings have their natural justification, we consider all of them. However, note that $k = 3$ is a special case because no matter which three slopes we pick, they can be affinely transformed to the slopes of the angles $\{45^\circ, 90^\circ, 135^\circ\}$ as illustrated in Fig. 2. Hence, we restrict considerations to this slope set. For illustrative purposes however, we often rotate drawings by 45° cw and thus use the slope set $\{\uparrow, \nearrow, \rightarrow\}$; see Fig. 1c.

A *k-slope assignment* of a digraph G assigns each edge of G one of k slopes. If G is upward plane, we call a *k-slope assignment* of G *consistent* if the assignment complies with the cyclic edge order around each vertex; e.g., for $k = 3$, if a vertex has three incoming edges, they need to be assigned the slopes \rightarrow , \nearrow , and \uparrow in counterclockwise (ccw) order. Clearly, if an upward plane embedding does not admit a consistent *k-slope assignment*, it also does not admit an upward planar *k-slope drawing*.

Contribution. We mainly contribute three results to the study of upward planar *k-slope drawings*. Firstly, we classify the upward planar slope numbers of directed ordered and unordered trees and show how to construct a drawing. Secondly, we show that for cactus graphs we can construct an upward planar *k-slope drawing* in polynomial time. Thirdly, we show that it is NP-hard to decide whether a given upward outerplanar digraph admits an upward planar 3-slope drawing. We extend the NP-hardness to $k > 3$ but restrict the graph class to upward planar (except for $k = 4$ if no embedding is given).

For statements marked with “ \star ”, a proof is available in the appendix.

2 Trees

In this section, we consider upward planar *k-slope drawings* of directed trees. While our trees are in general not rooted, results for rooted trees can be derived or are partially already known [2, 7]. For drawings of trees in the fixed and variable embedding scenario, the terms *ordered tree*, where a planar embedding is specified,

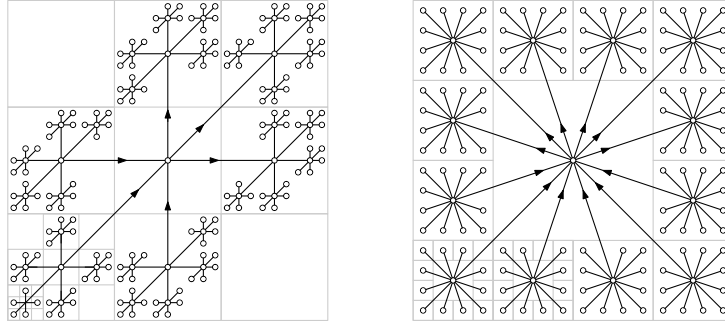


Fig. 3: Upward k -slope drawings of unordered tree $T_{3,3}$ with $k = 3$ and $T_{6,2}$ with $k = 6$, respectively, on the grid.

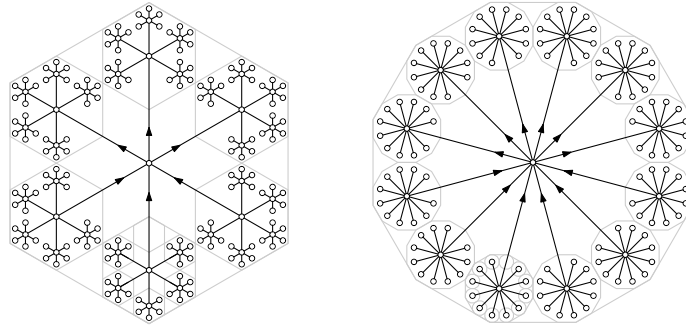


Fig. 4: Upward k -slope drawings of unordered tree $T_{3,3}$ with $k = 3$ and $T_{6,2}$ with $k = 6$, respectively, with uniform angles.

and *unordered* tree, where it is not, are used. Note that naturally every unordered tree is upward planar, while an ordered tree is upward planar if and only if its embedding is bimodal. Not surprisingly, the upward planar slope number of an unordered directed tree T equals the maximum in- and outdegree of T ; compare this to the planar slope number of $\lceil \Delta/2 \rceil$ of an unordered undirected tree with max. degree Δ [20]. To show this, we draw T as subgraph of a larger, regular tree $T_{k,h}$ for $h \geq 1$ where every non-leaf vertex has in- and outdegree k and each leaf has distance h to a central vertex. To draw $T_{k,h}$ on a grid with k slopes, we adopt the strategy of Bachmaier et al. [1] for complete rooted trees; see Fig. 3. Alternatively, $T_{k,h}$ can be drawn with k uniform angles; see Fig. 4.

Theorem 1 (\star). *Let T be an unordered directed tree with maximum indegree and outdegree k . Then T admits an upward planar k -slope drawing on the regular grid and another upward planar k -slope drawing with uniform angles.*

Note that this recursive drawing procedure requires an exponential-size drawing area (or an exponential edge-length ratio). Different from ordered directed trees (see below), it is not clear whether exponential area is necessary for some

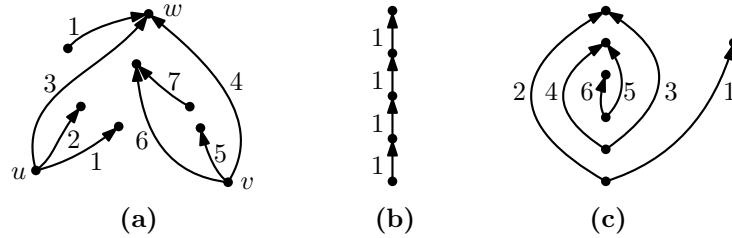


Fig. 5: (a) The minimal slope of an edge is not determined locally; (b) a directed path requires only one slope; (c) an alternating path requires $n - 1$ slopes.

unordered directed trees when restricting to k slopes. A $\Theta(n \log n)$ area suffices for an arbitrary number of slopes [22].

Next, let T be a bimodally ordered directed tree. With the drawing approach from unordered trees, it is clear that to determine the upward planar slope number of T it suffices to find a consistent k -slope assignment for T with minimal k . In this regard, note that the maximum in- and outdegree are natural lower bounds but that the choice of the (minimal) slope for an edge uv cannot be determined locally at u and v . For example, the edge vw in Fig. 5a is the third incoming edge at w but requires at least slope 4, since its preceding edge uw already requires slope 3 at u . This effect only appears along alternating intervals of incoming and outgoing edges. Hence we have the following observation – see also Fig. 5b–c.

Observation 2 *The upward planar slope number of ordered directed trees with n vertices, $n \geq 2$, is bounded within 1 and $n - 1$ and these bounds are tight.*

However, a simple greedy algorithm finds a consistent k -slope assignment for T , where k is minimal. The algorithm first identifies all edges that can have slope 1, e.g., if an edge uv is the sole incoming edge at v and the ccw first outgoing edge at u . Then, it gives any subsequent edge xy the maximum of the slope of its ccw preceding outgoing edge at x and its ccw preceding incoming edge at y plus one. Since linear time suffices for this and any additional bookkeeping, we get:

Theorem 3. *The upward planar slope number of an ordered directed tree can be determined in linear time.*

Corollary 1. *Let T be an ordered directed tree with maximum in-/outdegree k . We can decide in linear time whether T admits an upward planar k -slope drawing.*

Regarding the area requirement for k -slope drawings of ordered directed trees, we want to remark that Quapil and Jungeblut [39] have shown that there are ordered trees with a spiral structure that require exponential area for 3 slopes.

3 Cactus Graphs

In this section, we show that it can be decided in polynomial time whether a given cactus digraph admits an upward planar k -slope drawing, both in the fixed

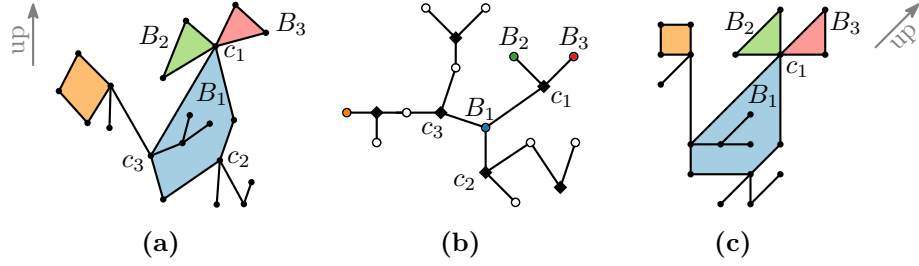


Fig. 6: (a) A cactus graph G ; (b) block-cut tree of G ; (c) 3-slope drawing of G .

and the variable embedding scenario. We use a dynamic program on the block-cut tree of the cactus that computes combinable k -slope assignments for each block.

Recall that a block-cut tree \mathcal{T} of a graph G has a vertex for each *block* (biconnected component) and each cut vertex of G and an edge between a block B and a cut vertex c if c is part of B ; see Fig. 6b. Let G be a cactus graph. Note that in a block-cut tree \mathcal{T} of G each block vertex is either a cycle or an edge – we thus distinguish between *cycle blocks* and *edge blocks*. The block-cut tree of G can be computed in linear time [40]. For G to admit an upward planar k -slope drawing, each block of \mathcal{T} must be drawable under constraints imposed by other blocks. For example in Fig. 6a–c and $k = 3$, under a fixed embedding the two edges of the block B_1 incident to the cut vertex c_1 need the slopes \nearrow and \uparrow because of the blocks B_2 and B_3 . Our strategy is thus as follows.

Algorithm. In the first phase we run a dynamic program (described below) on the blocks of \mathcal{T} to find a consistent slope assignment for each block such that the blocks are combinatorially combinable. If successful, we enter the second phase, where we compute drawings of the blocks that are geometrically combinable. In the last phase we put all block drawings together.

Let G be a cactus and let \mathcal{T} be the block-cut tree of G . We pick an arbitrary block vertex, say B' , of \mathcal{T} as root and direct all edges towards B' . As a result, each block vertex B (except B') has one outgoing edge towards a cut vertex c . We then say c is the *anchor* of B . Let B be a cycle block with anchor c and let e and e' be the edges of B incident to c . Suppose we have a slope assignment for B . Then the *anchor type* $t_c(B)$ of c for B is defined as the slopes of e and e' and if they are incoming or outgoing edges at c ; see Fig. 7. For an edge block B with edge e , the *anchor type* $t_c(B)$ describes the slope of e and if e is incoming or outgoing at c . For cycle blocks and edge blocks, there are $2k \cdot (2k - 1)$ and $2k$ different anchor types, respectively.

For a block vertex B with anchor c , a *feasible tuple* $\tau_B = \langle \phi_B, t_c(B) \rangle$ consists of a consistent k -slope assignment ϕ_B of B and an anchor type $t_c(B)$ of c . A *feasible set* for B is a maximal set of feasible tuples for B that have pairwise different anchor types. We process \mathcal{T} in a post-order traversal. For each block we compute the feasible set based on the feasible tuples of its descendant blocks.

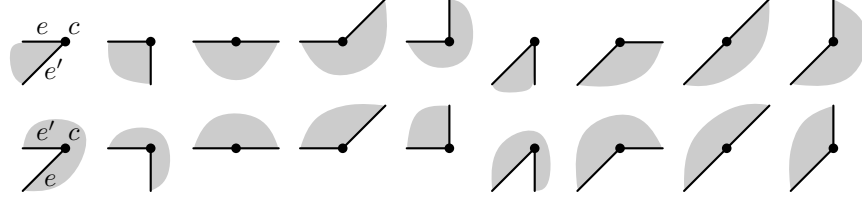
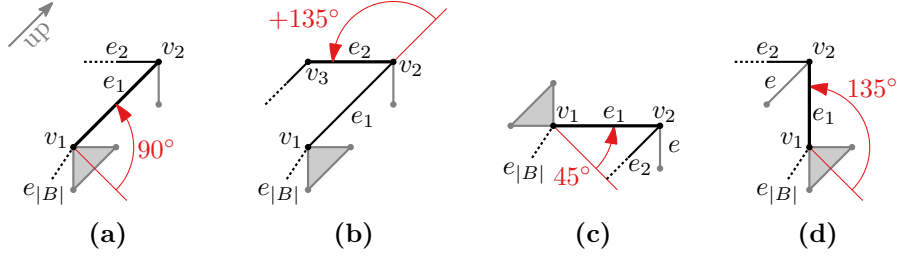
Fig. 7: A subset of the anchor types of a cycle block for $k = 3$.

Fig. 8: Computing the possible slopes and rotations for each edge of a cycle.

Combinatorial Realization. Computing the feasible set of a cycle block B with anchor c works as follows. Let B be the cycle $(c = v_1, e_1, v_2, e_2, \dots, v_{|B|}, e_{|B|}, v_1)$ – if an embedding is given, let the order be cw around the inner face. For every possible slope of e_1 , we walk around B once and store all tuples of possible slopes and how far we rotated from the start. We start with e_1 and consider the $\mathcal{O}(1)$ feasible tuples of descendant blocks of B anchored at v_1 and v_2 . In the example of Fig. 8a for $k = 3$, assuming a fixed embedding, the edge e_1 can only have slope \nearrow and we have thus rotated 90° (starting from the original x-axis). For this tuple $(\nearrow, 90)$, the edge e_2 in Fig. 8b has also only one possible slope, namely \rightarrow , and the rotation increases by 135° . However, in the variable embedding scenario, e_1 can also have slopes \rightarrow and \uparrow , see Fig. 8c–d. In general, for an edge e_i , $i \in \{2, \dots, |B|\}$, we consider for all tuples of e_{i-1} how e_i can proceed; again we consider the feasible tuples of descendant blocks of B at v_i and v_{i+1} . For each found tuple of e_i we store a pointer to the tuple(s) of e_{i-1} it is based on.

When we handle $e_{|B|}$, we reject all tuples that do not result in a 2π rotation if the embedding is given or with $\pm 2\pi$ if no embedding is given. This ensures that the cycle has a geometric realization [11]. Combining the slope of e_1 and $e_{|B|}$ as well as whether the rotation is $+2\pi$ or -2π yields an anchor type of B at c . We backtrack from the tuple of $e_{|B|}$ to find a consistent slope assignment of B .

Since the edge e_{i-1} can have at most $\mathcal{O}(k|B|)$ possible rotation values, which imply a slope each, we can compute all possible tuples of e_i in $\mathcal{O}(k|B|)$ time. Thus, a single feasible tuple of the whole block B can be computed in $\mathcal{O}(k|B|^2)$ time and all $\mathcal{O}(k)$ feasible tuples of B in $\mathcal{O}(k^2|B|^2)$ time.

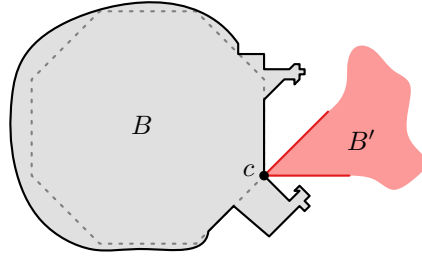


Fig. 9: When drawing a single block, we make sure that the anchor point c lies at a $2k$ -gon edge within the algorithm by Culberson and Rawlins [11]; here $k = 4$.

Geometric Realization. Suppose we have found a consistent k -slope assignment for every cycle. In the variable embedding scenario, we now know whether and how cycles nest. We thus re-root \mathcal{T} such that the root block lies on the outer face. Next, we describe how to obtain a drawing of a cycle block B as a polygon that does not intersect the edges of its parent block B' at its anchor point c .

We describe this only for the uniform angles setting and leave it as an open question for the regular grid setting. Given any sequence σ of rational angles (i.e., a rational number times π) that sum up to $\pm 2\pi$, Culberson and Rawlins [11] describe an algorithm that outputs a polygon with σ as turning angles. Internally, their so-called *Turtlegon* algorithm works as follows. It defines a base angle α as the greatest common divisor of π and all angles in σ ; in our case this is π/k . Larger angles are split into sequences of $\pm\alpha$ resulting in a new angle sequence σ' . W.l.o.g. let σ' contain more angles $+\alpha$ than $-\alpha$. Using some of the α s, their algorithm draws a regular $(2\pi/\alpha)$ -gon (in our case $2k$ -gon). To accommodate additional angles in between, it inserts exponentially shrinking detours at the corners of the $(2\pi/\alpha)$ -gon. In the end, we get the original larger angles from merging the smaller angles [11].

The difficulty for us when employing this $\mathcal{O}(k|B|)$ time algorithm, is to ensure that the edges of the parent block B' can reach the anchor point c without intersecting the polygon of B . This might be impossible if c lies within a spiral inside a detour. However, we can avoid this if we let an incident edge of c be a side of the $2k$ -gon (this is always possible because we can pick an appropriate set of α angles of σ' for the $2k$ -gon) and if we let each detour edge shrink by a sufficiently large factor (e.g., $k|B|$); see Fig. 9.

The running time of this step is in $\mathcal{O}(k|B|)$. Since each vertex is in at most k blocks, we have that $\sum_{i=1}^{\ell} |B_i| \leq kn$. Hence, the total running time is in $\mathcal{O}(k^2n)$.

Putting Blocks Together. We start with a drawing of the root block. We then recursively draw each child (in a BFS-like order) such that its anchor point coincides with the corresponding vertex of the parent polygon and scale down the drawing of the child block such that the appended polygon does not intersect the existing drawing. Note that it always suffices to scale down each child to the size of the minimum distance of any two vertices within in the parent polygon.

We can determine vertex pairs of minimum and maximum distance for a block B in $\mathcal{O}(|B| \log |B|)$ time and then place and scale each polygon in linear time.

The total running time is dominated by the dynamic program, which runs in $\mathcal{O}(k^2|B|^2)$ time for one block B and, hence, in $\mathcal{O}(k^4n^2)$ time for all blocks.

Theorem 4. *Let G be an upward planar (or plane) cactus graph with maximum in- and outdegree k . It can be constructively tested in $\mathcal{O}(k^4n^2)$ time whether G admits an upward planar k -slope drawing in the uniform angles setting.*

For the regular grid setting, we cannot use the algorithm by Culberson and Rawlins [11] because we have irrational multiples of π as turning angles. For a sequence of general turning angles, the algorithm by Hartley [24] computes a polygon realizing that sequence. However, it is not immediately clear how to guarantee that the edges of the parent polygon at the anchor point are not intersected. For general polygons, we believe that we can iteratively shrink the spikes to resolve potential intersections. Since such a procedure involves some more technicalities, we leave it as an open question for now.

4 Outerplanar and Planar Graphs

In this section, we show that for any constant $k \geq 3$ deciding whether an upward planar (for $k = 3$, outerplanar) digraph admits an upward planar k -slope drawing is NP-hard. Except for $k = 4$, this hardness holds true regardless of whether we prescribe an embedding or not. However, it remains open if the problem is also NP-complete. Containment in NP is not immediately clear, since it is open whether some graphs require irrational (or super-polynomial precise) coordinates for any k -slope drawing. We first describe our NP-hardness reduction for embedded outerplanar graphs for 3 slopes. Afterwards, we show how this extends to the variable embeddings and to larger k .

We reduce from PLANAR MONOTONE 3-SAT [4], an NP-complete version of 3-SAT, where the three literals of each clause are all either negated or unnegated – from now on called *negative* and *positive* clauses, respectively. Moreover, the incidence graph² has a planar drawing where the vertices are rectangles, the edges are vertical straight-line segments, the variables are arranged on a horizontal line, the positive clauses are above, and the negative clauses are below this line; see Fig. 11a. For a given formula F and a rectangular drawing of its incidence graph, we construct a corresponding upward outerplanar digraph G_F , which can only be drawn upward planar with 3 slopes if F is satisfiable. Our construction follows ideas of Nöllenburg [35] and Kraus [31] and utilizes the following observations.

Up to scaling and mirroring diagonally, G_\square in Fig. 10a admits an upward planar 3-slope drawing only as an outerplanar square as in Fig. 10b. We can attach multiple squares (and triangles) to each other as in Fig. 10c. The drawing

² The incidence graph of a SAT formula has a vertex for each variable and clause and an edge for each occurrence of a variable in a clause between the corresponding vertices.

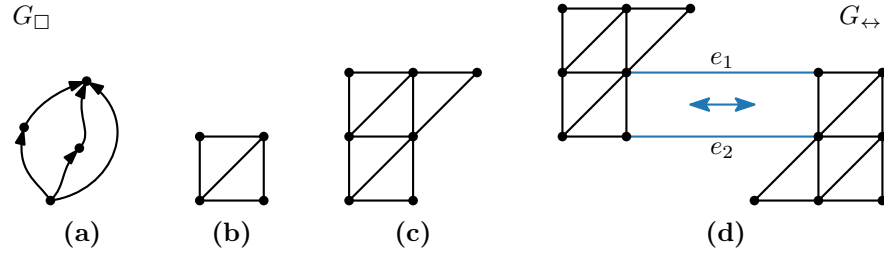


Fig. 10: (a) The digraph G_\square admits only an upward 3-slope drawing as square (b); (c) by combining copies of G_\square and triangles we can build larger rigid structures; (d) upward planar 3-slope drawing of the digraph G_{\leftrightarrow} .

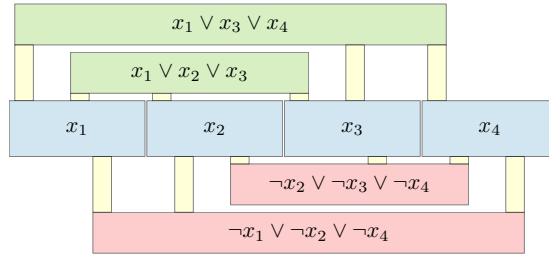
of such a bigger digraph is unique up to scaling and mirroring diagonally. If the squares form a tree, the drawing is outerplanar. We refer to these squares as *unit squares*, since, once set, the side lengths for all attached squares are the same. To allow a certain small degree of freedom, we exploit the following.

Lemma 1 (\star). *In any upward planar 3-slope drawing of G_{\leftrightarrow} (see Fig. 10d)*

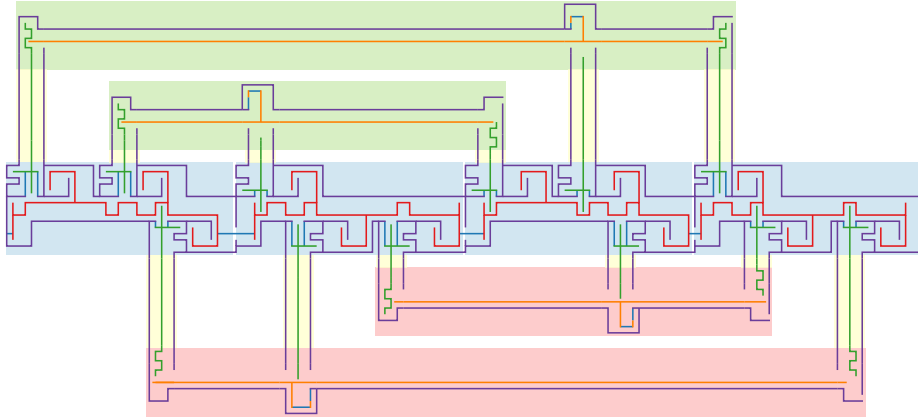
- the edges e_1 and e_2 are parallel and have the same arbitrary length $\ell > 0$,
- all edges are oriented as in Fig. 10d up to mirroring along a diagonal axis,
- and all vertical and horizontal edges (besides e_1 and e_2) have the same lengths, as well as all diagonal edges.

With this construction kit of useful (sub)graphs in hand, we build a graph whose upward planar drawings represent the satisfying truth assignments for F . The **high-level construction** is depicted in Fig. 11b. We construct, for each variable x_i , a specific digraph – the *variable gadget for x_i* . Similarly, for each clause c_j , there is a specific digraph – the *clause gadget for c_j* . All gadgets mainly consist of chains of G_\square s. For a drawing, this enforces a rigid frame structure built from unit squares. We glue all variable gadgets together in a row and connect variable and clause gadgets by *edge gadgets* such that the composite graph remains upward outerplanar (see Fig. 11b) and G_\square s are drawn as unit squares.

A **variable gadget** is depicted in Fig. 12. Its base structure is the (violet) **frame** composed of chains of unit squares. The core element is the (red) **central chain** of unit squares (with a few **side-arms**), which has one degree of flexibility, namely, moving as a whole to the left or to the right without leaving the **frame structure** of the gadget. It looks and behaves a bit like a pipe cleaning brush that is stuck inside the **frame** but can be moved a bit back and forth. Hence, we call it a **brush**. It is connected via a G_{\leftrightarrow} to the **brush** of the previous variable gadget (see Fig. 12a/d) and the first **brush** is connected to the **frame** via a G_{\leftrightarrow} . This allows only a horizontal shift of the **brushes**, but no vertical movement relative to its anchor point at the **frame structure**. Note that the horizontal position in any variable gadget is independent of those in all other gadgets. If the **brush** is positioned to the very left (right), the corresponding variable is set to false (true).



(a) Rectangular incidence graph drawing of a PLANAR MONOTONE 3-SAT formula F .



(b) Outerplanar drawing of the digraph G_F obtained from (a). Chains of unit squares are drawn as straight line segments. The variable/clause/edge gadgets occupy the areas of their corresponding rectangles. Here, x_1 and x_4 are set to false (**brush** on the left), while x_2 and x_3 are set to true (**brush** on the right)

Fig. 11: Schematic example for our NP-hardness reduction.

For each occurrence of a variable in a positive clause, we have a construction as depicted in Fig. 12b. There, a long chain of (green) G_{\square} s – from now on called **bolt** – is attached to the **frame structure** via two G_{\leftrightarrow} s, which allow only a vertical, but no horizontal shift. The **bolt** has on its left side an **arm**, which can only be placed in one of two **pockets of the frame**. It can always be placed in the **upper pocket**, which pushes the **bolt** outwards with respect to the variable gadget (into an edge and then a clause gadget). It can only be placed in the **lower pocket** if the **brush** is shifted to the very right (i.e. set to **true**) – then the **bolt** can “fall” into a cove of the **brush**. For each occurrence of a variable in a negative clause, we have this construction upside-down, such that the **bolt** can be pulled into the variable gadget only if the **brush** is shifted to the very left (i.e. set to false).

Note that, to maintain outerplanarity of the whole construction, the **frame structure** is not contiguous, but connected by G_{\leftrightarrow} s and the **arms** of the **bolts**. Hence, the **frame structure** decomposes into many components that have fixed

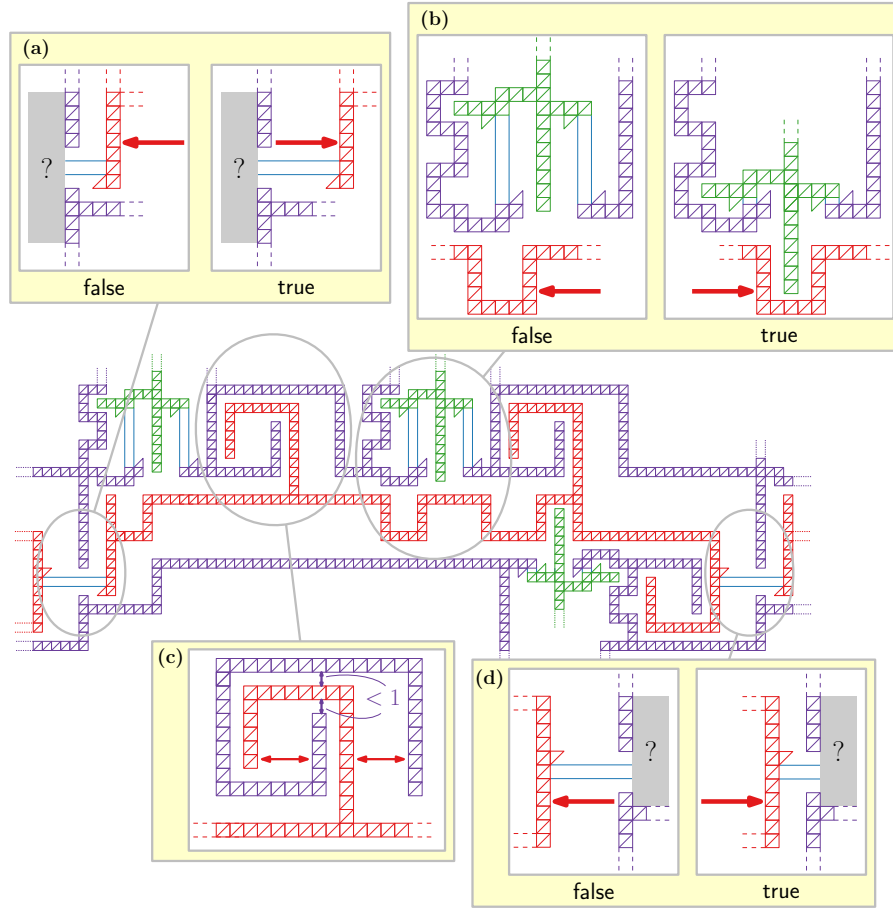


Fig. 12: A variable gadget, which is contained in two positive and one negative clauses. The **brush** is positioned to the left and, thus, the variable is set to false.

relative horizontal positions and their unit squares have the same side lengths. However, the components can shift up and down relative to each other. To keep this vertical shift small enough not to affect the correct functioning of our reduction, we use, for each such component, the construction depicted in Fig. 12c. The chain of **brushes** has no vertical flexibility and serves as a base ground for an “anchor” of the **frame**. The **frame** can move less than one unit up or down unless it violates planarity. If the **frame** would be shifted up enough to be completely above the **brush**, it would get in conflict with the adjacent **bolt**.

An **edge gadget** consists of only three straight chains – two **frame segments** and a **bolt** in the middle. Their purpose is to synchronize the distance of the clause gadgets to the variable gadgets and to preserve the size of the unit squares. Several edge gadgets are depicted on yellow background color in Fig. 11b.

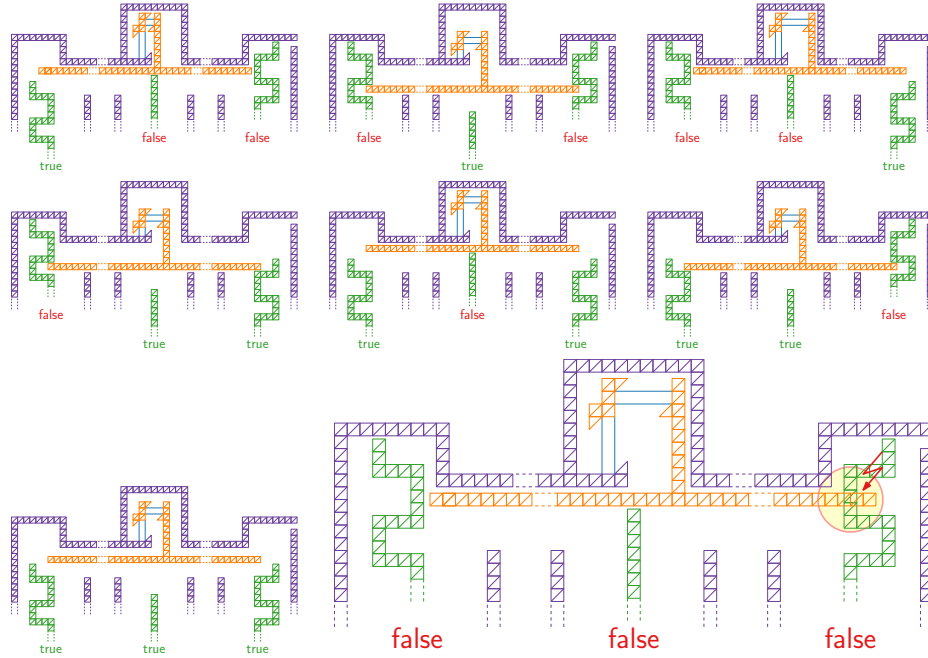


Fig. 13: Positive clause gadget in 8 configurations.

A **clause gadget** for a positive clause is depicted in Fig. 13. Within a **frame**, which is connected at six points to the **frames** of three edge gadgets, there is a horizontal (**orange**) **bar**, which is attached via two G_{\leftrightarrow} s to the **frame** – one G_{\leftrightarrow} allows a horizontal, the other allows a vertical shift. It resembles a crane that can move up and extend its arm, while it holds the horizontal **bar** on a vertical (**orange**) **rope**. The three **bolts** from the corresponding variable gadgets reach into the clause gadget. The lengths of these **bolts** is chosen such that, if they are pushed out of their variable gadget and into the clause gadget, they only slightly fit inside the gadget. Depending on whether each of the **bolts** is pushed into the clause gadget or pulled out of it, we have eight possible configurations (with sufficiently small vertical slack). They represent the eight possible truth assignments to a clause. In Fig. 13, we illustrate that in each configuration, we can accommodate the horizontal **bar** in an upward planar 3-slope drawing of the clause gadget – except for the case when all three **bolts** push into the clause gadget, which represents the truth assignment **false** to all contained variables. A negative clause gadget uses the same construction, but mirrored vertically.

Note that, since we have only connected G_{\square} s and G_{\leftrightarrow} s, the planar embedding of the constructed graph is unique up to mirroring along a diagonal axis. Therefore, our reduction holds true also for the variable embedding scenario and we conclude:

Theorem 5 (*). *Deciding whether an upward outerplanar digraph admits an upward planar 3-slope drawing is NP-hard with and without a given embedding.*

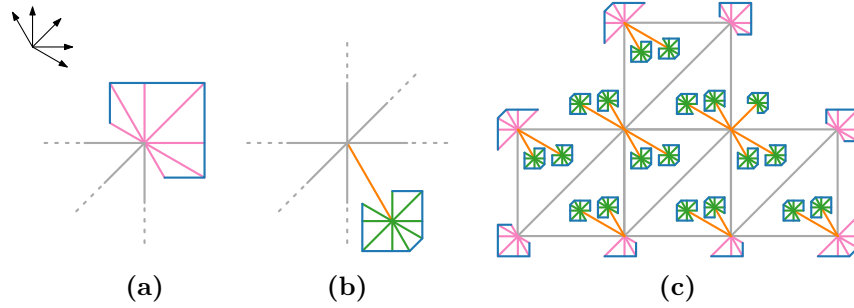


Fig. 14: Example for $k = 5$ slopes: (a) A fan and (b) a beater. (c) We add fans and beaters to each vertex of the graph such that all unused slopes are occupied.

Next, we describe how to extend our NP-hardness reduction to more than 3 slopes. There, however, we use only upward planar instead of upward outerplanar graphs. Observe that, if we fix the embedding and give up outerplanarity, we can add dummy leaves to each vertex to occupy all but the originally used slopes. Since any 3 slopes can be projected to $\{\uparrow, \nearrow, \rightarrow\}$ and we block all other slopes, our arguments work for all sets of k slopes and the reduction remains correct.

Last, we show that our NP-hardness reduction remains applicable for $k > 4$ in the variable embedding setting. This leaves $k = 4$ in the variable embedding setting as the only open case. Again, we do this by extending the graph such that it has only planar embedding up to mirroring along a diagonal axis.

Assume for now that k is an odd number; in the appendix, we consider otherwise. From the given k slopes, we pick the 3 middle slopes to host the graph of the hardness construction described before. For simplicity, we visualize these 3 middle slopes again as $\{\uparrow, \nearrow, \rightarrow\}$ and the other slopes in quadrants II and IV around a vertex. The key idea is to occupy the unused slopes at each vertex by *fans* and *beaters* as depicted in Fig. 14 instead of simple leaves. Fans are appended to the outside of each vertex if the angle that has been formed in the old construction is $\geq 180^\circ$. For each other remaining slope at each vertex, we add a beater. This is a graph obtained from the wheel graph W_{2k+1} of which one spoke e^* is broken free. This enforces an order on the spokes and, hence, we prescribe the slope of e^* . Note that the whole beater could be mirrored leaving two possible slopes for e^* . However, this is unproblematic since in our construction the “mirrored” slope is also occupied by a beater or a fan. In the appendix, we prove that this suffices to enforce a desired embedding. Though we lost upward outerplanarity, note that the underlying undirected graph remains outerplanar.

Theorem 6 (★). *Deciding whether an upward planar digraph with maximum in- and outdegree k admits an upward planar drawing with k slopes is NP-hard for $k \geq 3$ if a bimodal embedding is given and is NP-hard for $k \in \mathbb{N}^+ \setminus \{1, 2, 4\}$ if no embedding is given. This holds true for all choices of k slopes.*

References

1. Bachmaier, C., Brandenburg, F.J., Brunner, W., Hofmeier, A., Matzeder, M., Unfried, T.: Tree drawings on the hexagonal grid. In: Tollis, I.G., Patrignani, M. (eds.) Proc. of 16th Int. Symp Graph Drawing (GD'08). pp. 372–383. Springer (2008). https://doi.org/10.1007/978-3-642-00219-9_36
2. Bachmaier, C., Matzeder, M.: Drawing unordered trees on k -grids. *Journal of Graph Algorithms and Applications* **17**(2), 103–128 (2013). <https://doi.org/10.7155/jgaa.00287>
3. Bekos, M.A., Di Giacomo, E., Didimo, W., Liotta, G., Montecchiani, F.: Universal Slope Sets for Upward Planar Drawings. In: Biedl, T., Kerren, A. (eds.) Proc. of 26th International Symposium Graph Drawing & Network Visualization (GD'18). pp. 77–91 (2018). https://doi.org/10.1007/978-3-030-04414-5_6
4. de Berg, M., Khosravi, A.: Optimal binary space partitions for segments in the plane. *International Journal of Computational Geometry & Applications* **22**(3), 187–206 (2012). <https://doi.org/10.1142/s0218195912500045>
5. Bertolazzi, P., Di Battista, G., Liotta, G., Mannino, C.: Upward drawings of triconnected digraphs. *Algorithmica* **12**(6), 476–497 (1994). <https://doi.org/10.1007/BF01188716>
6. Bertolazzi, P., Di Battista, G., Mannino, C., Tamassia, R.: Optimal Upward Planarity Testing of Single-Source Digraphs. *SIAM Journal on Computing* **27**(1), 132–169 (1998). <https://doi.org/10.1137/S0097539794279626>
7. Brunner, W., Matzeder, M.: Drawing ordered $(k-1)$ -ary trees on k -grids. In: Brandes, U., Cornelsen, S. (eds.) Proc. of 18th International Symposium Graph Drawing & Network Visualization (GD'10). pp. 105–116. Springer (2011). https://doi.org/10.1007/978-3-642-18469-7_10
8. Brückner, G., Krisam, N.D., Mchedlidze, T.: Level-planar drawings with few slopes. In: Archambault, D., Tóth, C.D. (eds.) Proc. of 27th International Symposium Graph Drawing & Network Visualization (GD'19). pp. 559–572. Springer (2019). https://doi.org/10.1007/978-3-030-35802-0_42
9. Chan, H.: A Parameterized Algorithm for Upward Planarity Testing. In: Albers, S., Radzik, T. (eds.) Proc. of 12th Annual European Symposium on Algorithms (ESA'04). pp. 157–168 (2004). https://doi.org/10.1007/978-3-540-30140-0_16
10. Crescenzi, P., Di Battista, G., Piperno, A.: A note on optimal area algorithms for upward drawings of binary trees. *Computational Geometry* **2**(4), 187–200 (1992). [https://doi.org/10.1016/0925-7721\(92\)90021-J](https://doi.org/10.1016/0925-7721(92)90021-J)
11. Culberson, J.C., Rawlins, G.J.E.: Turtlegons: generating simple polygons for sequences of angles. In: Proc. of 1st Symposium on Computational Geometry (SoCG'85). pp. 305–310. ACM (1985)
12. Czyzowicz, J.: Lattice diagrams with few slopes. *Journal of Combinatorial Theory, Series A* **56**(1), 96–108 (1991). [https://doi.org/10.1016/0097-3165\(91\)90025-C](https://doi.org/10.1016/0097-3165(91)90025-C)
13. Czyzowicz, J., Pelc, A., Rival, I.: Drawing orders with few slopes. *Discrete Mathematics* **82**(3), 233–250 (1990). [https://doi.org/10.1016/0012-365X\(90\)90201-R](https://doi.org/10.1016/0012-365X(90)90201-R)
14. Di Battista, G., Eades, P., Tamassia, R., Tollis, I.G.: *Graph Drawing: Algorithms for the Visualization of Graphs*. Prentice-Hall (1999)
15. Di Battista, G., Tamassia, R.: Algorithms for plane representations of acyclic digraphs. *Theoretical Computer Science* **61**(2), 175–198 (1988). [https://doi.org/10.1016/0304-3975\(88\)90123-5](https://doi.org/10.1016/0304-3975(88)90123-5)
16. Di Giacomo, E., Liotta, G., Montecchiani, F.: Drawing outer 1-planar graphs with few slopes. *J. Graph Algorithms Appl.* **19**(2), 707–741 (2015). <https://doi.org/10.7155/jgaa.00376>

17. Di Giacomo, E., Liotta, G., Montecchiani, F.: Drawing subcubic planar graphs with four slopes and optimal angular resolution. *Theoretical Computer Science* **714**, 51–73 (2018). <https://doi.org/10.1016/j.tcs.2017.12.004>
18. Di Giacomo, E., Liotta, G., Montecchiani, F.: 1-bend upward planar slope number of SP-digraphs. *Computational Geometry* **90**, 101628 (2020). <https://doi.org/10.1016/j.comgeo.2020.101628>
19. Didimo, W., Giordano, F., Liotta, G.: Upward Spirality and Upward Planarity Testing. *SIAM Journal on Discrete Mathematics* **23**(4), 1842–1899 (2010). <https://doi.org/10.1137/070696854>
20. Dujmović, V., Eppstein, D., Suderman, M., Wood, D.R.: Drawings of planar graphs with few slopes and segments. *Computational Geometry* **38**(3), 194–212 (2007). <https://doi.org/10.1016/j.comgeo.2006.09.002>
21. Dujmović, V., Suderman, M., Wood, D.R.: Graph drawings with few slopes. *Computational Geometry* **38**(3), 181–193 (2007). <https://doi.org/10.1016/j.comgeo.2006.08.002>
22. Frati, F.: On minimum area planar upward drawings of directed trees and other families of directed acyclic graphs. *International Journal of Computational Geometry & Applications* **18**(03), 251–271 (2008). <https://doi.org/10.1142/S021819590800260X>
23. Garg, A., Tamassia, R.: On the Computational Complexity of Upward and Rectilinear Planarity Testing. *SIAM Journal on Computing* **31**(2), 601–625 (2001). <https://doi.org/10.1137/S0097539794277123>
24. Hartley, R.I.: Drawing polygons given angle sequences. *Inf. Process. Lett.* **31**(1), 31–33 (1989)
25. Healy, P., Lynch, K.: Two fixed-parameter tractable algorithms for testing upward planarity. *International Journal of Foundations of Computer Science* **17**(05), 1095–1114 (2006). <https://doi.org/10.1142/S0129054106004285>
26. Jelínek, V., Jelínková, E., Kratochvíl, J., Lidický, B., Tesař, M., Vyskočil, T.: The Planar Slope Number of Planar Partial 3-Trees of Bounded Degree. *Graphs and Combinatorics* **29**(4), 981–1005 (2013). <https://doi.org/10.1007/s00373-012-1157-z>
27. Keszegh, B., Pach, J., Pálvölgyi, D.: Drawing Planar Graphs of Bounded Degree with Few Slopes. *SIAM Journal on Discrete Mathematics* **27**(2), 1171–1183 (2013). <https://doi.org/10.1137/100815001>
28. Kindermann, P., Meulemans, W., Schulz, A.: Experimental analysis of the accessibility of drawings with few segments. *Journal of Graph Algorithms and Applications* **22**(3), 501–518 (2018). <https://doi.org/10.7155/jgaa.00474>
29. Klawitter, J., Mchedlidze, T.: Upward planar drawings with two slopes. *Arxiv report* (2021), <https://arxiv.org/abs/2106.02839>
30. Knauer, K., Micek, P., Walczak, B.: Outerplanar graph drawings with few slopes. *Computational Geometry* **47**(5), 614–624 (2014). <https://doi.org/10.1016/j.comgeo.2014.01.003>
31. Kraus, R.: Level-außenplanare Zeichnungen mit wenigen Steigungen (2020), Bachelor Thesis, University of Würzburg
32. Lenhart, W., Liotta, G., Mondal, D., Nishat, R.I.: Planar and Plane Slope Number of Partial 2-Trees. In: Wismath, S., Wolff, A. (eds.) *Proc. of 21st International Symposium on Graph Drawing (GD'13)*. pp. 412–423. Springer (2013). https://doi.org/10.1007/978-3-319-03841-4_36
33. Mukkamala, P., Pálvölgyi, D.: Drawing Cubic Graphs with the Four Basic Slopes. In: van Kreveld, M., Speckmann, B. (eds.) *Proc. of 19th International Symposium on Graph Drawing (GD'11)*. pp. 254–265. Springer (2011). https://doi.org/10.1007/978-3-642-25878-7_25

34. Makkamala, P., Szegedy, M.: Geometric representation of cubic graphs with four directions. *Computational Geometry* **42**(9), 842–851 (2009). <https://doi.org/10.1016/j.comgeo.2009.01.005>
35. Nöllenburg, M.: Automated Drawing of Metro Maps (2010), Diploma Thesis, University of Karlsruhe (TH)
36. Nöllenburg, M., Wolff, A.: Drawing and labeling high-quality metro maps by mixed-integer programming. *IEEE Transactions on Visualization and Computer Graphics* **17**(5), 626–641 (2011). <https://doi.org/10.1109/TVCG.2010.81>
37. Pach, J., Pálvölgyi, D.: Bounded-degree graphs can have arbitrarily large slope numbers. *Electronic Journal of Combinatorics* **13**(1), N1 (2006)
38. Papakostas, A.: Upward planarity testing of outerplanar DAGs. In: Tamassia, R., Tollis, I.G. (eds.) *Proc. of DIMACS International Workshop on Graph Drawing (GD'94)*. pp. 298–306 (1994). https://doi.org/10.1007/3-540-58950-3_385
39. Quapil, V.: Bachelor thesis on slope drawings. Karlsruhe Institute of Technology (2021), to appear; supervised by Jungeblut, P.
40. Tarjan, R.: Depth-first search and linear graph algorithms. *SIAM Journal on Computing* **1**(2), 146–160 (1972). <https://doi.org/10.1137/0201010>
41. Wade, G.A., Chu, J.H.: Drawability of Complete Graphs Using a Minimal Slope Set. *The Computer Journal* **37**(2), 139–142 (1994). <https://doi.org/10.1093/comjnl/37.2.139>

Appendix

Theorem 1. *Let T be an unordered directed tree with maximum indegree and outdegree k . Then T admits an upward planar k -slope drawing on the regular grid and another upward planar k -slope drawing with uniform angles.*

Proof. We draw T as subgraph of a larger, regular tree. More precisely, for $k \geq 3$ and $h \geq 1$, let $T_{k,h}$ be the balanced unrooted tree where every non-leaf vertex has indegree k and outdegree k and all leaves have distance h to a central vertex ρ . Let ℓ be a longest undirected path in T . If we find an upward planar k -slope drawing of $T_{k, \lceil \ell/2 \rceil}$, we obtain a drawing of T as subgraph of $T_{k, \lceil \ell/2 \rceil}$.

To draw $T_{k,h}$ on a grid with k slopes we adopt the strategy of Bachmaier et al. [1] for complete rooted trees; see Fig. 3. The vertex ρ is placed at the center of an axis-aligned square that functions as the drawing region. The neighbors of ρ are placed at the centers of smaller squares along the perimeter of the outer square. If k is even, we need $2k$ smaller squares and all are filled; if k is odd, we need $2(k+1)$ smaller squares where two stay empty. We then proceed recursively from the neighbors of ρ towards the leaf with ever smaller squares and thus shorter edge lengths.

Alternatively, to draw $T_{k,h}$ with k uniform angles, we use a regular $2k$ -gon as drawing region and use appropriately smaller regular $2k$ -gons for the subtrees; see Fig. 4. One corner of each smaller $2k$ -gon is incident with a corner of the larger $2k$ -gon and, for odd k , small $2k$ -gons touch at corners while, for even k , they touch at sides.

Lemma 1. *In any upward planar 3-slope drawing of G_{\leftrightarrow} (see Fig. 10d)*

- the edges e_1 and e_2 are parallel and have the same arbitrary length $\ell > 0$,
- all edges are oriented as in Fig. 10d up to mirroring along a diagonal axis,
- and all vertical and horizontal edges (besides e_1 and e_2) have the same lengths, as well as all diagonal edges.

Proof. As subgraphs, we have twice a pair of attached G_{\square} s. As observed before, each pair can only be drawn as attached unit squares. Without loss of generality,

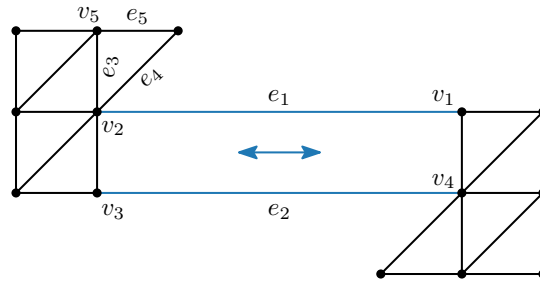


Fig. 15: Upward planar 3-slope drawing of the digraph G_{\leftrightarrow} as in Fig. 10d.

let the first two squares (containing vertices v_2, v_3, v_5) be drawn vertically above each other as in Fig. 15 (which is Fig. 10d in more detail). Since v_2 has outdegree 3 and e_3 has slope \uparrow , we can argue that the edge e_1 gets slope \rightarrow . If e_1 used \nearrow , the edge e_5 would have no slope to close the triangle (e_3, e_4, e_5) because, at v_5 , the rightmost outgoing slope is only \rightarrow . Thus, e_4 gets \nearrow and the only remaining slope for e_1 is \rightarrow . Note that e_3 is a unit square edge and the adjacent edges e_4 and e_5 use the same slopes as their counterparts in a unit square, giving them the corresponding lengths.

The same argument as for the outgoing edges of v_2 applies to the incoming edges of v_4 . However, assume for contradiction, that the whole block on the right side of Fig. 15 is mirrored diagonally, i.e., v_1 and v_4 are on the same horizontal line and e_2 gets slope \uparrow . Then, v_4, v_1 , and v_2 would be on the same horizontal line. This contradicts v_3 being vertically below its neighbors v_2 and v_4 . Hence, the right block has the same orientation as the left one, and e_2 gets slope \rightarrow and is parallel to e_1 . This implies that the distances between v_2 and v_3 on the one hand, and v_1 and v_4 on the other hand are the same and the G_{\square} s (and their attached triangles) have the size and orientation as in Fig. 15. By the orientation of v_1, v_2, v_3, v_4 , the edges e_1 and e_2 have an identical length ℓ . Only a value $\ell \leq 0$ would cause a non-planar drawing.

Theorem 5. *Deciding whether an upward outerplanar digraph admits an upward planar 3-slope drawing is NP-hard with and without a given embedding.*

Proof. To show NP-hardness, we use the reduction from PLANAR MONOTONE 3-SAT as described above. Let F be a given PLANAR MONOTONE 3-SAT formula with a rectangular drawing of the incidence graph of F and G_F be the digraph obtained by our reduction. Each gadget in G_F has only polynomial size and we can construct it in polynomial time.

If F is satisfiable, then there is a satisfying assignment T^* of truth values to the variables of F . Draw G_F as illustrated in Fig. 11b, Fig. 12, and Fig. 13 such that the **brush** in a variable gadget has a distance of ε (for some sufficiently small $\varepsilon > 0$) to the **frame** on its left if the corresponding variable is set to **false** in T^* and has a distance of ε to the **frame** on its right if the corresponding variable is set to **true**. This drawing uses only three slopes and is upward planar. Observe that it is also outerplanar. On a chain of unit squares, the vertices on both sides are incident to the outer face. The drawings of the variable gadgets are open from one to the other and the drawing of the rightmost variable gadget is open to the outside. Moreover, the drawings of the positive (negative) clause gadgets are open on their top (bottom) right and on their whole bottom (top) sides, which also gives the “covered” clause gadgets and the outer sides of the variable gadgets access to the outer face.

On the other hand, if there is an upward planar 3-slope drawing of G_F and it resembles the structure in Fig. 11b, we can read a satisfying truth assignment depending on the positions of the **brushes** (for the ones in intermediate position where no **bolt** can use the **lower pocket**, we can use any assignment for this variable).

In the remainder of this proof, we argue that any drawing resembles this structure. Consider the G_{\square} of the **frame structure** which is connected via a G_{\leftrightarrow} to the **brush** of the first variable gadget. Clearly, it is drawn as a unit square – it is our reference unit square having side length 1. Observe that all other unit squares are connected via chains of G_{\square} s or G_{\leftrightarrow} s to this reference unit square. By our observation and Lemma 1, they have the same side length. When ignoring the central parallel edges in the G_{\leftrightarrow} s, the drawing decomposes to few rigid components. The first rigid **frame component** contains the reference unit square. The central edges of the incident G_{\leftrightarrow} connecting it to the first **brush** can have only relatively small length as they would hit the “back wall” of, again, the first rigid **frame component** otherwise. Hence, the **brush** is indeed drawn inside the **frame** of the first variable gadget. Moreover, the first rigid **frame component** is connected via a G_{\leftrightarrow} to a **bolt**, which in turn is connected to the next rigid **frame components** of the first variable gadget (see Fig. 12b). Since this **bolt** cannot escape the upper boundary of the clause gadget, which is also part of the first rigid **frame component**, the **arm** is in one of the two **pockets**. Then, the start point of the next rigid **frame structure** cannot be above the **arm** of the **brush** in Fig. 12c and the construction depicted there keeps the vertical slack of this rigid **frame component** within the range $(-1, 1)$. This argument inductively propagates for all following rigid components. Hence, we have vertical slack of less than 1 for the **frame structures** and for the **arms** in the **pockets**. In the configuration false-false-false of the clause gadget, this would give us $2 - \varepsilon$ vertical gain if two **frames** move away from each other and $1 - \varepsilon$ gain if the **arm** is close to the bottom of its **pocket**. However, we would require a shift of the horizontal **bar** of more than 3 to be below or above the bulge of the left or the right **bolt**. Hence, this configuration is not drawable and all other positions of the horizontal **bar** correspond to one of the 7 other, satisfying configurations of Fig. 13.

Theorem 6. *Deciding whether an upward planar digraph with maximum in- and outdegree k admits an upward planar drawing with k slopes is NP-hard for $k \geq 3$ if a bimodal embedding is given and is NP-hard for $k \in \mathbb{N}^+ \setminus \{1, 2, 4\}$ if no embedding is given. This holds true for all choices of k slopes.*

Proof. In our construction using fans and beaters, every vertex has in- and outdegree k and, hence, every available slope at each vertex needs to be used. Consequently, if we prescribe the embedding, this already determines the precise slope for each edge. Since we occupy all but three slopes with fans and beaters, which can also be drawn arbitrarily small, the reduction from Theorem 5 holds true also for $k > 3$. Clearly, the graph remains upward planar, but it is not upward outerplanar any more.

Now consider the case where we only prescribe the graph but no embedding. Again, for $k = 3$ we can use Theorem 5. Now assume that $k > 3$ is an odd number. We will consider the case where k is even afterwards. We show next that the extended graph can only be embedded in the desired previously described way up to mirroring along a diagonal axis.

Observe that the (pink) edges of each fan occupy neighboring slopes because their other endpoints are connected by (blue) edges. For every fan, the slope

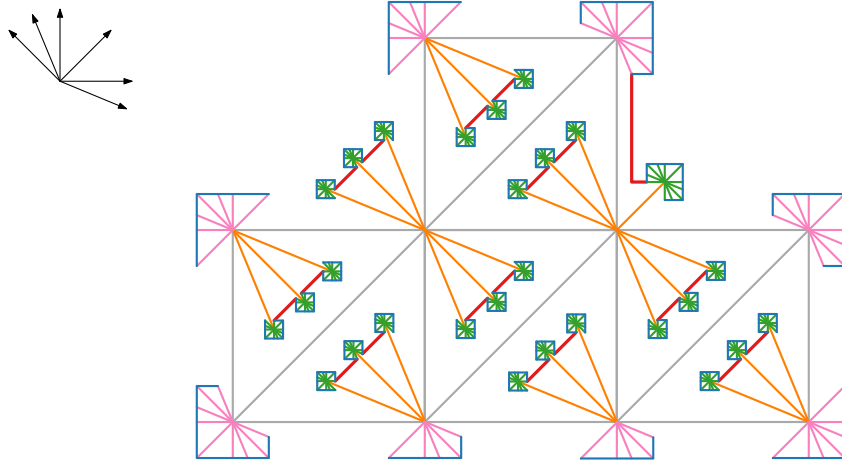


Fig. 16: Example for $k = 6$ slopes, where we have added (red) dummy edges to connect the beaters to each other or an adjacent fan, which fixes the faces, in which the beaters end up, in the case k is even and greater than 4.

set it covers contains both incoming and outgoing edges. Therefore, there are at most two ways to add a fan to a vertex – either to its left or to its right side. In any case, it needs to be added to the outer face since otherwise neither a G_{\square} nor a G_{\leftrightarrow} can be drawn (any fan blocks $\geq k - 1$ slopes, which corresponds to $\geq 180^\circ$).

The inner (green) edges of a beater occupy all but one slope, which remains for the (orange) edge connecting the beater to its vertex. Again, because of the switch between incoming and outgoing edges, the (orange) connecting edge needs to use one of two possible slopes – say the ℓ -th or the $(k - \ell + 1)$ -th slope. Since k is an odd number, the middle slope $\ell = \lceil k/2 \rceil$ is unique, which fixes the position of some beaters. For the other beaters, observe that we use the $(\lceil k/2 \rceil - 1)$ -th and the $(\lceil k/2 \rceil + 1)$ -th slope never for a beater, but always for the edges of the original construction. For all other values of ℓ , the opposite $(k - \ell + 1)$ -th slope is always occupied by another beater or a fan.

This means, given the embedding in the graph of the reduction of Theorem 5 is unique up to mirroring, the embedding of the extended graph is unique up to mirroring and exchanging the positions of pairs of beaters.

It remains to consider the case when $k > 4$ is even. Our goal is to use for the graph from Theorem 5 always the same 3 middle slopes, e.g., the $(k/2 - 1)$ -th, $k/2$ -th, and $(k/2 + 1)$ -th slope as in Fig. 16. This is automatically the case, if all fans and beaters are drawn in the desired face. We next describe how we can enforce in which face a beater or fan is drawn. At each vertex, we connect all incident beaters that shall share a common face by dummy edges as depicted by the thick red edges in Fig. 16. If there is only one beater at a vertex at a face, we connect it by two edges to a neighboring fan; see the on the top right of

Fig. 16. This latter case concerns only beaters on the outer face that block the slope \nearrow . (Inside a G_{\leftrightarrow} , we do not need beaters in between e_1 and e_2 .) In every other case, observe that within each bundle of connected beaters being adjacent to a vertex v , there is at least one beater being connected to v by an outgoing edge, and there is at least one beater being connected to v by an incoming edge. Hence, this bundle must be placed in the face being incident to v where the direction of bounding edges switches. This is either the opposite side of a fan or the opposite side of another bundle of beaters. In the latter case, the bundle of beaters cannot be exchanged since this would leave an incoming and an outgoing slope unused, which is not possible if v has in- and outdegree k .

Finally note that even for this construction with the additional connecting (red) edges, the underlying undirected graph remains outerplanar.